Received: 28 April 2022 | Revised: 25 June 2022 | Accepted: 28 June 2022

DOI: 10.1111/iwj.13895

ORIGINAL ARTICLE

IWJ WILEY

Changes in miroRNA-103 expression in wound margin tissue are related to wound healing of diabetes foot ulcers

Xiaotong Zhao | **Murong Xu** | **Ying Tang** | **Dandan Xie** | **Youmin Wang** | **Mingwei Chen**

Department of Endocrinology, the First Affiliated Hospital of Anhui Medical University, Hefei, People's Republic of China

Correspondence
Prof. Youmin Wang and Prof. Mingwei Chen, Department of Endocrinology, the First Affiliated Hospital of Anhui Medical University, 210 JiXi Road, Hefei, Anhui 230032, People's Republic of China.
Email: 971359183@qq.com and chmw1@163.com

Funding information
the Natural Science Foundation of Anhui Province in China, Grant/Award Number: 2108085MH269; the Natural Science Research Project of Colleges and Universities in Anhui Province, Grant/Award Number: KJ2021A0274

Abstract

To investigate the relationship between small noncoding microRNA-103 (miR-103) and wound healing of diabetic foot ulcers (DFU) and the underlying molecular mechanism, forty type 2 diabetes mellitus with DFU (DFU group), and 20 patients with a chronic skin ulcer of lower limbs and normal glucose tolerance (SUC group) were included. Quantitative real-time PCR method was used to determine miR-103 expression levels in the wound margin tissue of subjects, and to analyse the relationship between the expression of miR-103 and DFU wound healing. In vitro experiments were also performed to understand the effect of miR-103 on the high glucose-induced injury of normal human dermal fibroblasts (NHDFs) cells. The results showed that the miR-103 expression level in the DFU group was significantly higher than that in the SUC group [5.81 (2.25–9.36) vs 2.08 (1.15–5.72)] ($P < 0.05$). The expression level of miR-103 in the wound margin tissue of DFU was negatively correlated with the healing rate of foot ulcers after four weeks ($P = 0.037$). In vitro experiments revealed that miR-103 could inhibit the proliferation and migration of NHDF cells and promote the apoptosis of NHDF cells by targeted regulation of regulator of calcineurin 1 (RCAN1) gene expression in a high glucose environment. Downregulation of miR-103 could alleviate high glucose-induced NHDF cell injury by promoting RCAN1 expression. Therefore, the increased expression of miR-103 is involved in the functional damage of NHDF cells induced by high-glucose conditions, which is related to poor wound healing of DFU. These research findings will provide potential targets for the diagnosis and treatment of chronic skin wounds in diabetes.

KEYWORDS

foot ulcer, human dermal fibroblasts, miR-103, RCAN1, type 2 diabetets

Xiaotong Zhao and Murong Xu contributed equally to this study.

Key Messages

- microRNAs (miRNAs) are involved in the regulation of wound healing
- to investigate the relationship between miR-103, wound healing of diabetic foot ulcers (DFU), and the underlying molecular mechanism, forty type 2 diabetes mellitus with DFU (DFU group), 20 patients with chronic skin ulcer of lower limbs, and normal glucose tolerance (SUC group) were included
- in vitro experiments were performed to understand the effect of miR-103 on the high glucose-induced injury of human dermal fibroblasts cells
- the increased expression of miR-103 in wound margin tissue of DFU may be associated with poor wound healing
- the miR-103 is involved in the high glucose-induced functional impairment in dermal fibroblasts through targeted regulation of regulator of calcineurin 1 (RCAN1) expression

1 | INTRODUCTION

Diabetic foot ulcer (DFU) is a common, serious, chronic complication of diabetes mellitus. It is estimated that 19–34% of patients with diabetes are likely to be affected by a DFU in their lifetimes, and the International Diabetes Federation reports that 9.1–26.1 million diabetic patients will develop DFUs annually.[1,2] A one-year observational cohort study of 1333 diabetic patients aged over 50 in eight hospitals in China showed that the annual incidence of DFU was 8.1%.[3] DFU is one of the main reasons for non-traumatic foot amputation. As a result of the adverse effects of a high-glucose environment and abnormal changes in the skin microenvironment in diabetic patients, DFU has delayed healing or is difficult to repair and becomes chronical wounds that are difficult to heal.[4]

Normal skin is mainly composed of keratinocytes, fibroblasts, and extracellular matrix. Fibroblasts are the most important cells in wound healing.[5] Hyperglycaemia reduces the expression of integrin receptors on the surface of rat dermal fibroblasts and the migration capacity of these cells.[6] In vitro studies on human primary dermal fibroblasts also suggested that high glucose could significantly reduce the migration capacity of fibroblasts, thereby affecting wound healing.[7] Hyperglycaemia can reduce the proliferative capacity of dermal fibroblasts, change the cell cycle distribution, and accelerate the occurrence of G0/G1 phase arrest, cell senescence, and death.[8,9] Lafosse et al.[10] found that the ability of dermal fibroblasts to secrete cytokines that promote wound healing decreased in a high-glucose environment. In addition, long-term hyperglycaemia can cause abnormal metabolism and dysfunction of human dermal fibroblasts.[11] Clinical and animal studies have found that the proliferation and migration capacity of fibroblasts from chronic ulcers in diabetic subjects significantly decreased.[12,13] The above studies all suggested that hyperglycaemia can damage the function of skin fibroblasts, thus affecting wound healing.

MicroRNAs (miRNAs) are a class of endogenous non-coding small RNAs that regulate the expression of genes and/or proteins at the posttranscriptional level and participate in a variety of biological processes, including cell proliferation, apoptosis, cell cycle progression, and differentiation.[14] In the skin of neonatal mice, the absence of the Dicer or DGCR8 gene required for miRNA biosynthesis can lead to defects in the skin barrier function, follicular dysplasia, and excessive proliferation of epidermal basal cells, indicating that miRNA plays an important role in skin development and maintenance of skin function.[15,16] Etich J et al.[17] found that during wound healing, the expression of some miRNAs, including miR-103, significantly changed, and these miRNAs may be involved in regulating wound healing. Animal studies have shown that miR-103-3p in goat skin tissue plays an important role in the regulation of the hair follicle cycle.[18] In vitro experiments revealed that miR-103 regulates the late stages of autophagy in human keratinocytes.[19] Additionally, an increasing number of reports outlined the involvement of miR-103 in the proliferation, migration, invasion, and apoptosis of tumour cells.[20,21] It was believed that wound healing and tumours were similar in molecular and functional mechanisms.[22] These results suggest that miR-103 may participate in the process of wound healing.

TargetScan predicts that the regulator of calcineurin 1 gene (RCAN1) may be a target gene of miR-103 and involved in the development of many diseases.[23-25] Studies have shown that RCAN1 can antagonise the mitochondrial breakage and oxidative damage of rat glomerular mesangial cells induced by high glucose,[26] and its reduced expression is related to the abnormal mitochondrial function in patients with type 2 diabetes.[27,28] Knockout of the RCAN1 gene can aggravate

proteinuria and podocyte injury in mice with adriamycin-nephropathy.[29] Recent studies have revealed that RCAN1 can regulate the NF-κB signalling pathway, thereby participating in the process of skin inflammation.[30] The up-regulated expression of RCAN1 in vascular endothelial cells can promote the integrity of the vascular endothelial barrier and reduce vascular permeability.[31] Gimeno et al.[32] studied fibroblasts of foetuses with Down syndrome and found that down-regulation of RCAN1 expression could lead to increased oxidative stress, decreased proliferative capacity, and impaired cellular functions of fibroblasts. Therefore, RCAN1 is essential to maintain the normal functions of various cells, especially against disordered cell functions caused by high glucose.

In addition, there is a general sense that dermal fibroblasts play an important role in skin immunity and skin inflammation. They can produce a variety of cytokines dealing with inflammatory responses and regulation of immune function, such as interleukin-6 (IL-6), IL-10, tumour necrosis factor α (TNF-α), interferon-γ (IFN-γ), and monocyte chemotactic proteins, induce inflammatory cell infiltration, and ultimately lead to local inflammation, which may be involved in the regulation of wound healing.[33,34]

At present, a large quantity of clinical and animal studies have confirmed that the expression of miR-103 in the peripheral blood of type 2 diabetic rats and patients is up-regulated,[35-37] which participates in the insulin signalling pathway, insulin resistance and metabolic regulation.[38] However, the research on whether miR-103/RCAN1 is involved in wound healing of DFU has not been published. Thus, the main purposes of this study are: (1) To investigate whether the expression of miR-103 and RCAN1 in the wound margin tissue of DFU is different from that in the wound margin tissue of non-diabetes lower limb chronic skin ulcer, and to explore the relationship between the expression of miR-103 in the wound margin tissue of DFU and the wound healing of DFU; (2) To probe the expression changes of miR-103 and RCAN1 in fibroblasts under a high-glucose environment in vitro; (3) To determine whether miR-103 directly targets RCAN1, thereby affecting the changes of fibroblast proliferation, migration or apoptosis in the high-glucose environment. Based on these studies, we expect to preliminarily understand the relationship between miR-103 and the healing of DFU and its molecular mechanisms.

2 | MATERIALS AND METHODS

2.1 | Study subjects

A total of 40 patients with type 2 diabetes associated with DFU who were hospitalised in the Department of Endocrinology, the First Affiliated Hospital of Anhui Medical University, between April 2020 and December 2020, had a course of foot ulcer ≥4 weeks, an ankle-brachial index (ABI) of 0.9–1.3, an ulcer area within 2–20 cm^2 and a Wagner classification at II-III grade (DFU group). Besides, the skin ulcer control group (SUC group) consisted of 20 patients with skin ulcers of the lower limbs with normal glucose tolerance and was matched with the DFU group in terms of age and gender. They were hospitalised in the Burns Department of the First Affiliated Hospital of Anhui Medical University during the same period of enrollment and had no lower extremity arterial or vein lesions, and the duration of the ulcer was ≥4 weeks. All subjects had no severe heart, liver, or kidney dysfunction or cancerous ulcer wounds. The study was approved by the Medical Ethics Committee of the First Affiliated Hospital of Anhui Medical University, and all participants provided informed consent.

2.2 | Study methods

2.2.1 | Collection of ulcer margin tissue samples and treatment of diabetic foot ulcer

As described by the previous study,[39] all the subjects underwent wound debridement after admission. During the debridement process, the full-sickness skin tissue within 0.5 cm of the wound margin was cut by skilled surgeons using tissue scissors according to the sampling protocol. Meanwhile, all DFU patients were given routine systemic treatment, including anti-infection treatment, antihypertensive treatment, hypoglycemic treatment, correction of hypoproteinemia, neuroprotection treatment, etc. The changes in wound condition in DFU patients were followed up. The wound healing of the DFU patients was recorded after 4 weeks of treatment.

2.2.2 | Detection of observational indexes

Venous blood was drawn from the elbow of each subject at 8:00 to 8:30 AM on the morning after a 10-h fast, and was collected into anticoagulant tubes or non-anticoagulant tubes for determination of fasting plasma glucose (FPG), glycosylated haemoglobin A1c (HbA1c), white blood cell count (WBC), C-reactive protein (CRP), and other indicators. FPG was detected by the glucose oxidase method, HbA1c by high-pressure liquid chromatography, and CRP by latex-enhanced scattering immunoturbidimetric assay. Ulcer area was measured by digital photography combined with Image J medical image analysis software (Image J-ij133-jdk15; National Institutes of Health,

Bethesda, MD, USA), and ABI was measured by Doppler blood flow detector (DPL-03; Hangzhou Yuanxiang Medical Equipment Co., Ltd, China).

2.2.3 | Cell culture

Primary normal human dermal fibroblasts (NHDFs) were purchased from the Cell Resource Center of the Institute of Basic Medical Sciences of the Chinese Academy of Medical Sciences. NHDFs were cultured in RPMI 1640 medium (Gibco, USA) containing 10% FBS (Gibco, USA) and two antibodies and placed in a 37°C and 5% CO_2 incubator. Cells were passaged and cultured for 10 to 14 d, and the medium was replaced once every 2 to 3 d. Cells after the 6th generation were used for subsequent experiments. Before the experiment, serum was starved for 24 h to synchronise the cells.

2.2.4 | Grouping

Synchronised NHDFs were harvested and inoculated into 6-well plates for high-glucose intervention. After intervention with high glucose (25 mM) for 6 h, 12 h, or 24 h, the apoptosis rate of each group of NHDFs was examined. The appropriate concentrations were screened for subsequent experiments. Experimental groups included the NC group (5 mmol/L D-glucose), HG 6 h group (25 mM D-glucose intervention for 6 h), HG 12 h group (25 mM D-glucose intervention for 12 h), and HG 24 h group (25 mM D-glucose intervention for 24 h). Groups for testing the effect of interfering with miR-103 expression on the proliferation, migration, and apoptosis of high glucose-treated NHDFs and secretion of inflammatory cytokines by high glucose-treated NHDFs included the HG + anti-miR-con group (NHDFs were transfected with anti-miR-con for 24 h and cultured in medium containing high glucose (25 mM) for 12 h) and the HG + anti-miR-103 group (NHDFs were transfected with anti-miR-103 for 24 h and cultured in medium containing high glucose (25 mM) for 12 h). The experimental groups for testing the regulation of RCAN1 expression by miR-103 included the miR-con group (NHDFs were transfected with miR-con for 24 h), the miR-103 group (NHDFs were transfected with miR-103 mimic for 24 h), the anti-miR-con group (NHDFs were transfected with anti-miR-con for 24 h) and the anti-miR-103 group (NHDFs were transfected with anti-miR-103 for 24 h). The groups for testing the effect of RCAN1 overexpression on the proliferation, migration, and apoptosis of high glucose-treated NHDFs and their secretion of inflammatory cytokines included the HG + pcDNA group (NHDFs were transfected with pcDNA for 24 h and cultured in a medium containing high glucose (25 mM) for 12 h) and the HG + pcDNA-RCAN1 group (NHDFs were cultured in medium containing high glucose (25 mM) for 12 h after transfection with pcDNA-RCAN1 for 24 h). The groups for testing the effects of interfering with RCAN1 expression and interfering with a miR-103 expression on the proliferation, migration, and apoptosis of high glucose-treated NHDFs and secretion of inflammatory cytokines by high glucose-treated NHDFs included the HG + anti-miR-103 + si-con group (NHDFs were co-transfected with anti-miR-103 and si-con for 24 h and cultured in medium containing high glucose (25 mM) for 12 h) and the HG + anti-miR-103 + si-RCAN1 group (NHDFs were co-transfected with anti-miR-103 and si-RCAN1 for 24 h and cultured in medium containing high glucose (25 mM) for 12 h).

2.2.5 | Detection of the proliferative capacity of NHDFs

Proliferative capacity of NHDFs was measured using the CCK-8 kit (Beyotime, Shanghai, China). The cells of each group were digested with 0.25% trypsin (Sigma, USA) in the logarithmic growth phase, inoculated into 96-well plates at 2000 cells/well, and incubated overnight. The medium was refreshed. Ten microliters of CCK-8 solution were added to each well, and the cells were incubated in a 37°C and 5% CO_2 incubator for 2 h. Dimethyl sulfoxide was added after aspirating the supernatant, and the plates were shaken for 10 min. The optical density (OD) of each well was measured at 450 nm using a microplate reader.

2.2.6 | Detection of the migration capacity of NHDFs

After digestion with 0.25% trypsin, cells in each group were collected and diluted in a serum-free medium, and the cell concentration was adjusted to 2×10^5 cells/mL. Then, 100 μL of cell suspension was added into the upper chamber of the Transwell chamber (Corning, USA), 600 μL of medium containing 10% FBS was added into the lower chamber, and the plate was incubated at 37°C for 12 h. The Transwell chambers were removed, and the culture medium was discarded. The cells were washed with phosphate-buffered saline (PBS) twice, fixed in 4% paraformaldehyde for 15 min, air-dried at room temperature, and stained with 0.1% crystal violet for 30 min. The unmigrated cells in the upper layer were gently wiped off

with cotton swabs and washed with PBS three times. Five microscopic fields were randomly selected to count the number of migrated cells.

2.2.7 | Detection of apoptosis of NHDFs using flow cytometry

Cells were collected from each group, washed with precooled PBS, digested with 0.25% trypsin, centrifuged at 10000 r/min for 5 min at 4°C, washed with PBS, added to 1 mL of binding buffer, and centrifuged at 10000 r/min for 5 min at 4°C. The supernatant was discarded. The cells were added to 200 μL of binding buffer, 5 μL of annexin V-fluorescein isothiocyanate-propidium iodide, incubated at room temperature in the dark for 20 min, added to 400 μL of binding buffer, and loaded into the flow cytometer to measure the apoptosis rate. Cells were detached and labelled using an Annexin V-FITC/propidium iodide (PI) apoptosis detection kit (BestBio Co., Ltd., Shanghai, China) according to the manufacturer's instructions. Cells that were Annexin V+/PI– were indicative of early apoptosis, and are shown in the lower right quadrant of the FACS histogram, whereas cells that were Annexin V+/PI+ were considered to be late apoptotic cells, and are shown in the upper right quadrant of the FACS histogram. Apoptosis rate = early apoptotic cells (Annexin V+/PI–)+ late apoptotic cells (Annexin V+/PI +)/total cells.

2.2.8 | Detection of miR-103 and RCAN1 expression by quantitative real-time PCR assays

Quantitative real-time PCR assays (qRT-PCR) were performed to detect the expression of miR-103 and RCAN1 in wound margin tissue and NHDFs. RNA was extracted from 50 mg of wound margin tissue or cultured NHDFs according to the instructions of the miRcute miRNA extraction and separation kit (TaKaRa, Tokyo, Japan). cDNA was then synthesised according to the instructions of miRcute miRNA cDNA synthesis kit (GenePharma, Shanghai, China). The primer sequences of miR-103 and RCAN1 were as follows: miR-103: forward primer 5′-AG AGCCTGTGGTGTCCG-3′ and reverse primer 5′-CATCT TCAAAGCACTTCCCT-3′; U6: forward primer 5′-CTCG CTTCGGCAGCACA-3′ and reverse primer 5′-AACGCTT CACGAATTTGCGT-3′; RCAN1: forward primer 5′-GAC TGGAGCTTCATCGACTGC-3′ and reverse primer 5′-CA GCCTTGCCTTGACCATCT-3′; β-actin: forward primer 5′-AGCTGAGAGGGAAATCGTGC-3′ and reverse primer 5′-ACCAGACAGCACTGTGTT-3′.

qRT-PCR was carried out according to the instructions of the miRcute miRNA fluorescence quantitative detection kit (GenePharma, Shanghai, China). The cycling conditions for miR-103 were: initial denaturation at 95°C for 5 min, denaturation at 95°C for 20 s, annealing at 60°C for 40 s, and extension at 72°C for 30 s, for a total of 40 cycles. With U6 as the internal reference, the relative expression of miR-103 was calculated based on the $2^{-\Delta\Delta Ct}$ method. In addition, the cycling conditions for RCAN1 were: initial denaturation at 95°C for 2 min, denaturation at 95°C for 30 s, annealing at 60°C for 50 s, and extension at 74°C for 30 s, for a total of 40 cycles. With β-actin as the internal reference, the relative expression of RCAN1 mRNA was calculated based on the $2^{-\Delta\Delta Ct}$ method.

2.2.9 | Detection of RCAN1, Bax, and Bcl-2 by Western blotting

The NHDFs in each group were added to lysis buffer (Beijing Dingguo Changsheng Biotechnology Co. Ltd., China) and lysed for 30 min, and the total protein was extracted after centrifugation. The protein concentration was determined by the bicinchoninic acid (BCA) method (Beyotime, Shanghai, China). The denatured protein was subjected to sodium dodecyl sulfate–polyacrylamide gel electrophoresis. For electrophoresis, 30 μg of protein was run per well and transferred to membranes. The membranes were blocked with 5% non-fat milk at room temperature for 2 h, added to the dilution of the primary antibody (Abcam, USA) against RCAN1 (dilution: 1:500), Bax (dilution: 1:500), Bcl-2 (dilution: 1:500) at 4°C overnight. Subsequently, the membranes were incubated with the appropriate horseradish peroxidase-conjugated secondary antibody (dilution: 1:1000; Beijing Zhongshan Golden Bridge Biotechnology Co., Ltd., China) at room temperature for 1 h. Then, the developer (Thermo Fisher Scientific, Inc.) was added dropwise for development, and pictures were taken. β-actin was used as the internal reference protein to calculate the relative expression of the proteins.

2.2.10 | Detection of IL-6 and TNF-α levels in cell culture medium by enzyme-linked immunosorbent assay (ELISA)

The cell culture medium of each group was collected and the IL-6 and TNF-α levels were measured in strict accordance with the instructions of the respective ELISA kits (Shanghai Jianglai Biotechnology Co., Ltd., China).

2.3 | Luciferase reporter gene assay

TargetScan predicted the presence of a miR-103 binding site in the 3′UTR of RCAN1. The 3′UTR fragment of RCAN1 containing binding sites and mutation sites was inserted into the PGL3 luciferase reporter vector to construct the wild-type vector WT-RCAN1 and the mutant vector MUT-RCAN1. miR-con and miR-103 were transfected into the NHDF cells with WT-RCAN1 or MUT-RCAN1. The NHDFs were continuously cultured in a 37°C incubator for 48 h and then collected. A Pierce™ Firefly Luciferase Glow Assay Kit (Promega, USA) was used to detect luciferase activity in each group.

2.4 | Statistical analysis

SPSS version 22.0 (IBM SPSS Company, USA) was used for the statistical analysis. Normal measurement data is expressed by mean ± standard deviation, and nonnormal measurement data is expressed by median (interquartile range) [M(P25, P75)]. The *t*-test was used to analyse differences between two groups, and the comparison between multiple groups used the analysis of variance test, followed by the SNK-q test. The count data was expressed as a percentage, and the χ^2 test was performed. Spearman correlation analysis was used to evaluate the correlation between the expression of miR-103 in wound margin tissue and other clinical variables. All statistical tests were two-sided, and $P < 0.05$ represents a significant difference. Each in vitro independent experiment was repeated at least three times.

3 | RESULTS

3.1 | Comparison of clinical data between DFU group and SUC group

The expression of miR-103 in the wound margin tissue (T-miR-103), FPG, HbA1c levels were significantly increased in the DFU group compared with the SUC group ($P < 0.05$), yet RCAN1 mRNA expression in the wound margin tissue (T-RCAN1) was markedly decreased in the DFU group compared with the SUC group ($P < 0.05$). No obvious differences were found between the DFU and SUC groups in terms of gender, age, ulcer duration, ulcer area, ABI, CRP, WBC ($P > 0.05$). The detailed results are shown in Table 1.

3.2 | Correlations between miR-103 level in wound margin tissue and other clinical data

As shown in Table 2, in the DFU group, T-miR-103 level was positively correlated with FPG, and HbA1c levels ($P < 0.05$). While T-miR-103 level was negatively correlated with T-RCAN1 level in both DFU and SUC groups ($P < 0.05$). There was no significant correlation between T-miR-103 level and other indicators in the two groups ($P > 0.05$).

TABLE 1 Comparison of clinical data between DFU group and SUC group [$(\bar{x} \pm s)$, M (P25, P75)]

Variable	DFU (n = 40)	SUC (n = 20)	*P* value
Sex (male/female)	40 (22/18)	20 (11/9)	0.674
Age (year)	52.6 ± 8.5	51.7 ± 7.9	0.106
Ulcer duration (week)	6.8 ± 2.4	6.6 ± 2.5	0.351
Ulcer area (cm^2)	10.7 ± 3.6	9.9 ± 3.9	0.165
FPG (mmol/L)	10.5 ± 3.3	5.2 ± 0.7	<0.001
HbA1c (%)	9.4 ± 1.4	5.3 ± 0.3	<0.001
ABI	1.0 ± 0.1	1.1 ± 0.1	0.101
CRP (mg/dl)	30.5 ± 2.4	29.8 ± 1.9	0.182
WBC ($\times 10^9$)	9.2 ± 2.2	8.7 ± 1.8	0.136
T-miR-103	5.81 (2.25–9.36)	2.08 (1.15–5.72)	<0.001
T-RCAN1	0.69 (0.23–1.19)	1.26 (0.78–2.15)	0.003

Note: Data presented as mean ± SD or median with IQR. Differences between two groups analysed using *t* test or χ^2 test.
Abbreviations: ABI, ankle brachial index; CRP, C-reactive protein; DFU, diabetic foot ulcer; FPG, fasting plasma glucose; HbA1c, glycated haemoglobin A1c; SUC, skin ulcer control with normal glucose tolerance; T-miR-103, miR-103 expression in the wound margin tissue; T-RCAN1, RCAN1 mRNA expression in the wound margin tissue; WBC, white blood cell count.

3.3 | Relationship between miR-103 level in wound margin tissue and the clinical features of diabetic foot ulcers

To further investigate the clinical significance of altered miR-103 expression level, the median wound margin tissue miR-103 expression level of DFU patients was used as the cut-off point for grouping, namely, the low expression group (lower than the cut-off point) and the high expression group (higher than or equal to the cut-off point). Comparison of the clinical characteristics of ulcers between the two groups showed that miR-103 expression levels were negatively correlated with the healing rate of foot ulcers after 4 weeks ($P = 0.037$). No significant correlation was observed between the miR-103 expression level and other clinical features of foot ulcers (Table 3).

3.4 | Expression of miR-103 and RCAN1 in NHDFs under high-glucose intervention at different time points

NHDFs were intervened with high glucose for 6, 12 and 24 h. Compared with the NC group, the protein and mRNA expression levels of RCAN1 in NHDFs in the HG 6 h group (at 6 h), HG 12 h group (at 12 h) and HG 24 h group (at 24 h) were significantly decreased ($P < 0.05$, Figure 1A-C). On the contrary, the expression levels of miR-103 in the NHDFs in the HG 6 h group, HG12 h group and HG 24 h group were markedly increased compared with the NC group ($P < 0.05$, Figure 1D).

3.5 | Changes in the proliferation, migration, and apoptosis of NHDFs and secretion of inflammatory cytokines by NHDFs under high-glucose treatment at different time points

Under high-glucose intervention, compared with the NC group, the apoptosis rate of NHDFs (Figure 2A,B), the intracellular Bax protein expression levels (Figure 2C,D), both IL-6 levels (Figure 2H) and TNF-α levels (Figure 2I) in cell culture medium in the HG 6 h group, HG12 h group and HG 24 h group were significantly increased ($P < 0.05$). Conversely, compared with the NC group, the intracellular Bcl-2 protein expression levels (Figure 2C,E),

TABLE 2 Correlations between T-miR-103 expression level and other clinical data in the DFU group and SUC group (*r*)

	DFU (n = 40)		SUC (n = 20)	
Variables	***r***	***P* value**	***r***	***P* value**
Age	0.057	0.467	0.041	0.595
Sex	0.037	0.651	0.055	0.478
Ulcer duration	0.139	0.112	0.102	0.241
Ulcer area	0.096	0.296	0.068	0.402
FPG	0.314	0.002	0.179	0.082
HbA1c	0.338	0.001	0.192	0.067
ABI	−0.078	0.379	0.082	0.301
CRP	0.131	0.119	0.112	0.197
WBC	0.127	0.125	0.115	0.183
T-RCAN1	−0.394	<0.001	−0.325	0.003

Abbreviations: ABI, ankle brachial index; CRP, C-reactive protein; DFU, diabetic foot ulcer; FPG, fasting plasma glucose; HbA1c, glycated haemoglobin A1c; SUC, skin ulcer control with normal glucose tolerance; T-miR-103, miR-103 expression in the wound margin tissue; T-RCAN1, RCAN1 mRNA expression in the wound margin tissue; WBC, white blood cell count.

TABLE 3 Relationship between the expression levels of miR-103 in wound margin tissue and the clinical features of DFU patients [$(\bar{x} \pm s)$, n (%)]

	High expression group (n = 24)	Low expression group (n = 16)	*P* value
Age (year)	51.5 ± 7.9	52.7 ± 8.2	0.674
Sex			0.897
Male	13 (54.2)	9 (56.3)	
Female	11 (45.8)	7 (43.7)	
Ulcer area (cm^2)			0.912
≤5	4 (16.7)	2 (12.5)	
5 ~ 10	15 (62.5)	10 (62.5)	
>10	5 (20.8)	4 (25.0)	
Ulcer duration (week)			0.562
≤6	4 (16.7)	4 (25.0)	
6 ~ 10	14 (58.3)	10 (62.5)	
>10	6 (25.0)	2 (12.5)	
Wagner grade			0.693
II	9 (37.5)	7 (43.8)	
III	15 (63.5)	9 (56.2)	
Ulcer healing rate after 4 weeks (%)			0.037
Healing	7 (29.2)	10 (62.5)	
Non-healing	17 (70.8)	6 (37.5)	

Note: Data are presented as mean ± standard deviations or numbers (%); Differences between two groups analysed using *t* test or x^2 test. The cut-off point of miR-103 expression level for grouping was 5.81.
Abbreviations: DFU, diabetic foot ulcer.

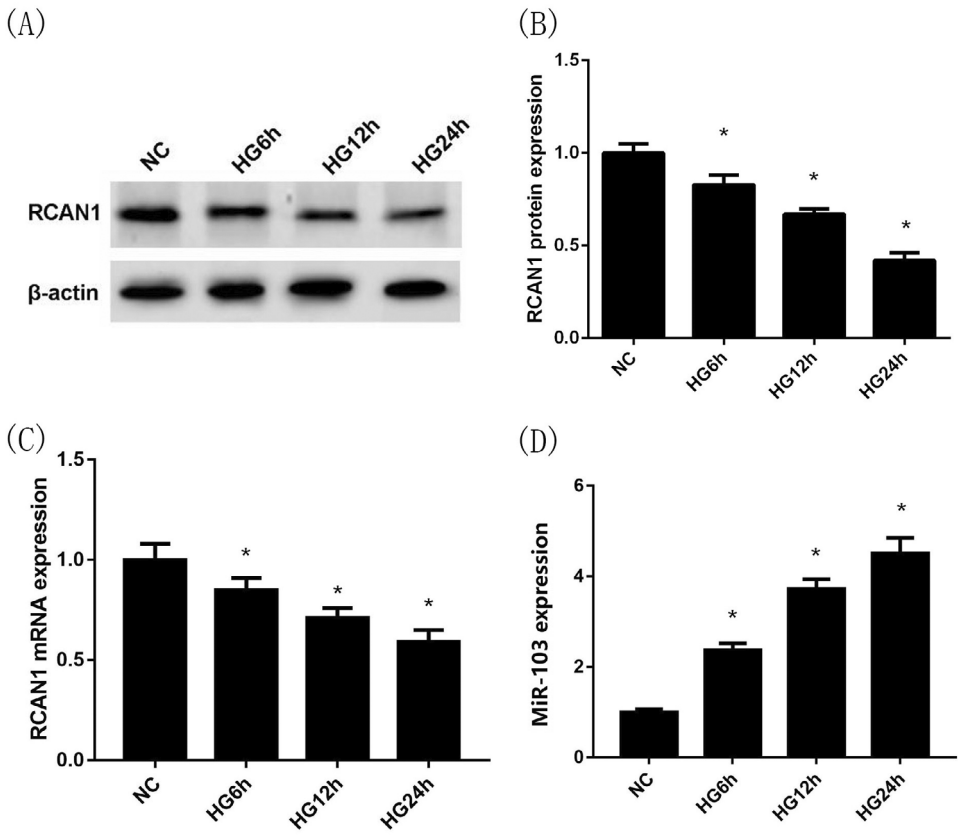

FIGURE 1 Expression of miR-103 and RCAN1 in NHDFs at 6, 12 and 24 h under high glucose intervention. Compared with the NC group, the protein expression levels of RCAN1 by Western blotting (A),(B) and the mRNA expression levels of RCAN1 by qRT-PCR (C) in NHDFs in the HG 6 h group (at 6 h), HG 12 h group (at 12 h) and HG 24 h group (at 24 h) were significantly decreased. By contrast, compared with the NC group, the miR-103 expression levels in NHDFs (D) in the HG 6 h group, HG12 h group and HG 24 h group were markedly increased. *$P < 0.05$ vs the NG group; n = 3 in each group. NG, normal glucose; HG, high glucose; NHDFs, human dermal fibroblasts; RCAN1, regulator of calcineurin 1

proliferation and migration capacities of NHDFs (Figure 2F,G) in the HG 6 h group, HG12 h group and HG 24 h group were dramatically decreased ($P < 0.05$). Among them, the HG 12 h group (treatment at 12 h) had the best effect, so it was selected for subsequent experiments.

3.6 | Inhibition of miR-103 expression reverses the effects of high-glucose treatment on the proliferation, migration, and apoptosis of NHDFs and their secretion of inflammatory cytokines

Compared with the NC group, the apoptosis rate of NHDFs and the level of miR-103 expression in the HG group were significantly higher ($P < 0.05$, Figure 3A,B,C). Moreover, the level of Bax protein expression was increased and the Bcl-2 was decreased ($P < 0.05$, Figure 3D,E,F). Similarly, after intervention with high glucose, the capacities of proliferation and migration of NHDFs were statistically lower than that of the NC group ($P < 0.05$, Figure 3G,H), and the levels of IL-6 and TNF-α in the cell culture medium were obviously higher than that of the NC group ($P < 0.05$, Figure 3I,J). Then NHDFs were transfected with anti-miR-con and anti-miR-103 for 24 h under high-glucose intervention, respectively, the results showed that the apoptosis rate of NHDFs and the level of miR-103 expression in the HG + anti-miR-103 group was significantly decreased compared with the HG + anti-miR-con group ($P < 0.05$, Figure 3A,B,C), indicating that the transfection was successful. In additional, compared with the HG + anti-miR-con group, the intracellular Bax protein expression levels in the HG + anti-miR-103 group was decreased ($P < 0.05$, Figure 3D,E) while the intracellular Bcl-2 protein expression levels was increased ($P < 0.05$, Figure 3D,F). At the same time, NHDFs in the HG + anti-miR-103 group had higher proliferation and migration capacities ($P < 0.05$, Figure 3G,H), and IL-6 and TNF-α protein levels in cell culture medium decreased significantly compared with the HG + anti-miR-con group ($P < 0.05$, Figure 3I,J).

3.7 | Targeted regulation of RCAN1 expression by miR-103

TargetScan predicted that miR-103 with WT-RCAN1 but not MUT-RCAN1 had complementary nucleotide sequences (Figure 4A). NHDFs were transfected with miR-con and miR-103 mimics, anti-miR-con and anti-miR-103 for 24 h, respectively, the results showed that the protein expression level of RCAN1 in the miR-103

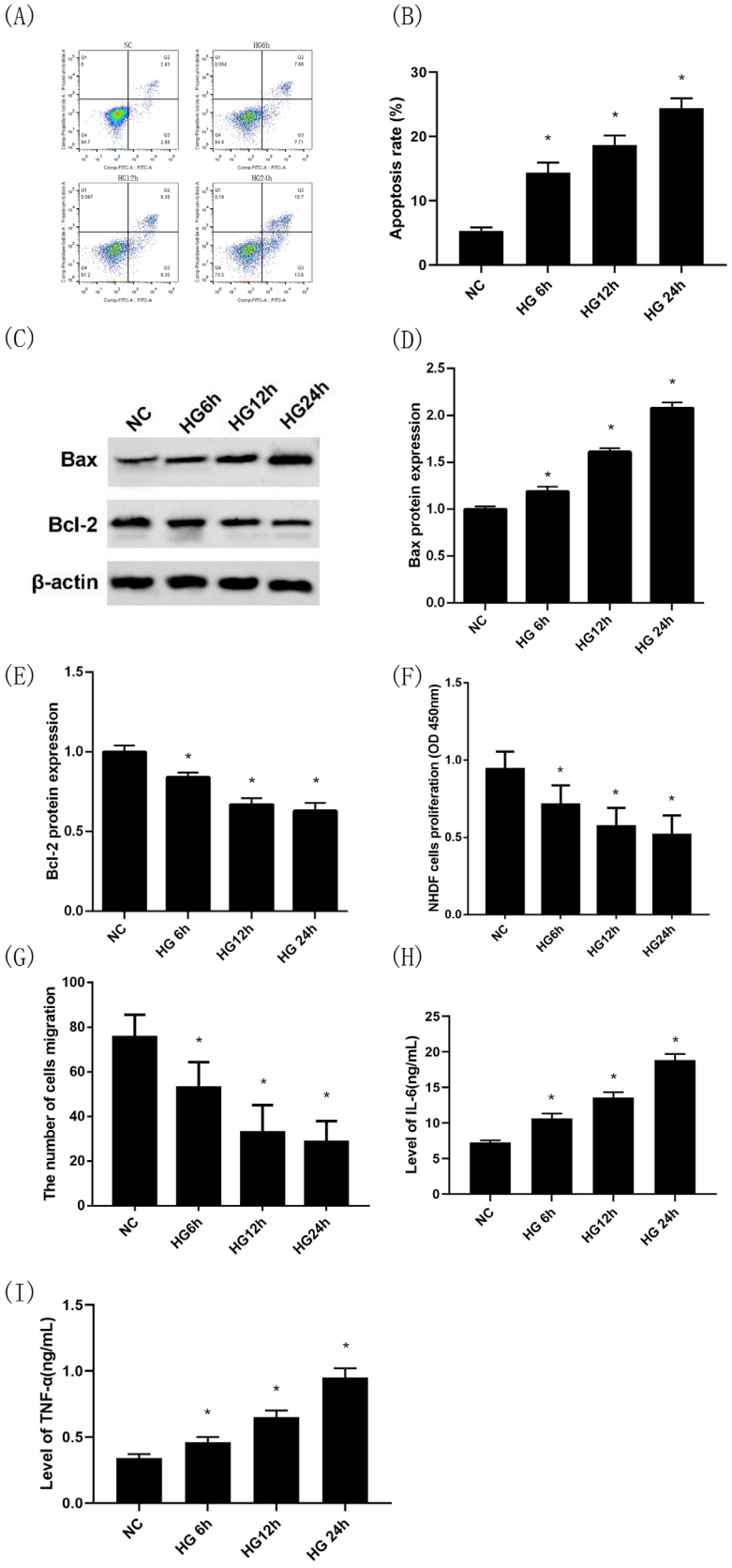

FIGURE 2 Changes in the proliferation, migration, and apoptosis of NHDFs and secretion of inflammatory cytokines by NHDFs under high-glucose treatment at different time points. Apoptosis of NHDFs under high-glucose intervention at different time points by flow cytometry (Annexin V-PI) (A),(B); Bax protein expression under high-glucose intervention at different time points by Western blotting (C),(D); Bcl-2 protein expression under high-glucose intervention at different time points by Western blotting (C),(E); Proliferation capacity of NHDFs under high-glucose intervention at different time points by CCK-8 (F); The number of cells migration of NHDFs under high-glucose intervention at different time points by transwell migration assay (G); IL-6 levels in cell culture medium under high-glucose intervention at different time points by ELISA (H); TNF-α levels in cell culture medium under high-glucose intervention at different time points by ELISA (I); *$P < 0.05$ vs the NG group; n = 3 in each group. NG, normal glucose; HG, high glucose; NHDFs, human dermal fibroblasts

group was lower than that of the miR-con group, and the protein expression level of RCAN1 in the anti-miR-103 group was higher than that of the anti-miR-con group ($P < 0.05$, Figure 4B,C). Moreover, the results of the dual-luciferase reporter gene assay showed that there was no significant difference in luciferase activity between the

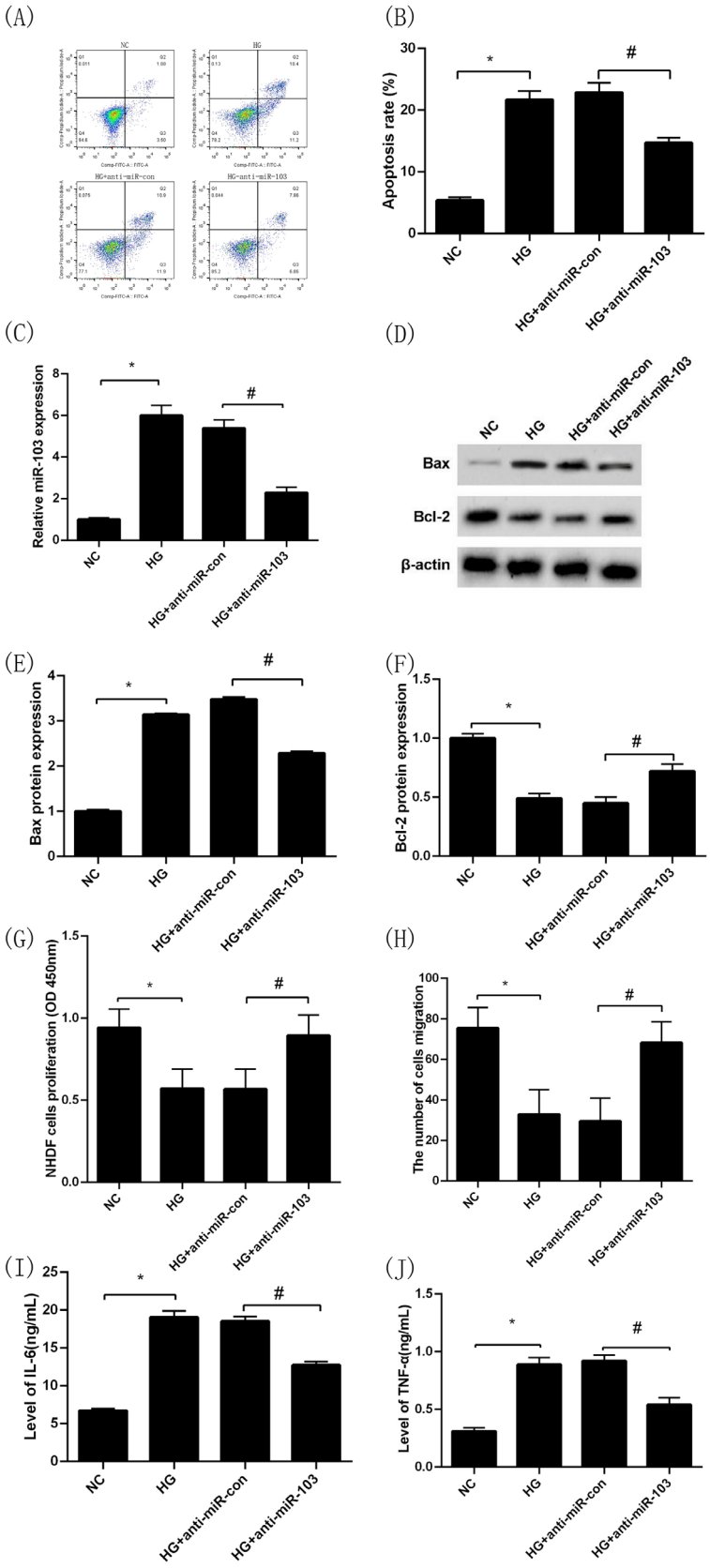

FIGURE 3 Inhibition of miR-103 expression reverses the effects of high-glucose treatment on the proliferation, migration, and apoptosis of NHDFs and their secretion of inflammatory cytokines. Apoptosis of NHDFs in NC, HG, HG + anti-miR-con and HG + anti-miR-103 groups by flow cytometry (Annexin V-PI) (A), (B); MiR-103 expression in NC, HG, HG + anti-miR-con and HG + anti-miR-103 groups by qRT-PCR (C); Bax protein expression in NC, HG, HG + anti-miR-con and HG + anti-miR-103 groups by Western blotting (D),(E); Bcl-2 protein expression in NC, HG, HG + anti-miR-con and HG + anti-miR-103 groups by Western blotting (D), (F); Proliferation capacity of NHDFs in NC, HG, HG + anti-miR-con and HG + anti-miR-103 groups by CCK-8 (G); The number cells of migration of NHDFs in NC, HG, HG + anti-miR-con and HG + anti-miR-103 groups by transwell migration assay (H); IL-6 levels in cell culture medium in NC, HG, HG + anti-miR-con and HG + anti-miR-103 groups by ELISA (I); TNF-α levels in cell culture medium in NC, HG, HG + anti-miR-con and HG + anti-miR-103 groups by ELISA (J). *$P < 0.05$ vs the NG group, $^{\#}P < 0.05$ vs the HG + anti-miR-con group; n = 3 in each group. NG, normal glucose; HG, high glucose; NHDFs, human dermal fibroblasts

miR-103 group and the miR-con group after transfection of the MUT-RCAN1-3′UTR vector plasmid ($P > 0.05$, Figure 4D), while after transfection of with the WT-RCAN1-3′UTR vector plasmid, the luciferase activity of the miR-103 group was significantly lower than that of the miR-con group ($P < 0.05$, Figure 4D).

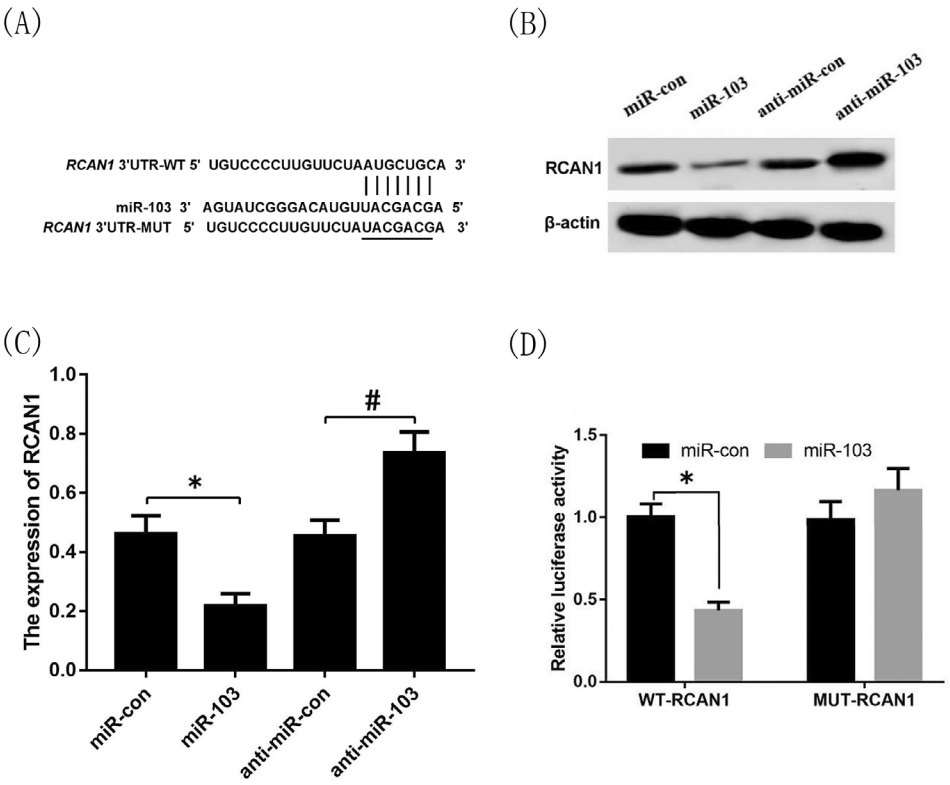

FIGURE 4 Targeted regulation of RCAN1 expression by miR-103. The miR-103 and RCAN1 had complementary nucleotide sequences (A); The protein expression of RCAN1 in miR-con, miR-103, anti-miR-con and anti-miR-103 groups (B),(C); The luciferase activity of miR-103 group and miR-con group after transfection of the RCAN1-3'UTR WT and MUT vector plasmid (C). $^{*}P < 0.05$ vs the miR-con group, $^{\#}P < 0.05$ vs the anti-miR-con group. n = 3 in each group. WT, wild-type; MUT, mutant-type; RCAN1, regulator of calcineurin 1

3.8 | Overexpression of RCAN1 inhibits the effects of high glucose on the proliferation, migration, and apoptosis of NHDFs and secretion of inflammatory cytokines by NHDFs

Similar to the above results, the apoptosis rate of NHDFs in the HG group was significantly higher while the level of RCAN1 protein expression was dramatically lower compared with the NC group ($P < 0.05$, Figure 5A-D). Moreover, the level of Bax protein expression was increased and the Bcl-2 was decreased ($P < 0.05$, Figure 5C,E,F). Similarly, after intervention with high glucose, the capacities of proliferation and migration of NHDFs were significantly lower than that of the NC group ($P < 0.05$, Figure 5G,H), and the levels of IL-6 and TNF-α in the cell culture medium were markedly higher than that of the NC group ($P < 0.05$, Figure 5I,J). Then, NHDFs were transfected with pcDNA and pcDNA-RCAN1 for 24 h under high-glucose intervention, respectively, the results showed that the apoptosis rate of NHDFs was decreased and the level of RCAN1 protein expression was increased in the HG + pcDNA-RCAN1 group compared with the HG + pcDNA group ($P < 0.05$, Figure 5A-D), indicating that the transfection was successful. In additional, compared with the HG + pcDNA group, the intracellular Bax protein expression levels in the HG + pcDNA-RCAN1 group was decreased ($P < 0.05$, Figure 5C,E) and the intracellular Bcl-2 protein expression levels was increased ($P < 0.05$, Figure 5C,F). At the same time, NHDFs in the HG + pcDNA-RCAN1 group had higher proliferation and migration capacities ($P < 0.05$, Figure 5G,H), and IL-6 as well TNF-α levels in cell culture medium significantly decreased compared with the HG + pcDNA group ($P < 0.05$, Figure 5I,J).

3.9 | Inhibition of RCAN1 expression reverses the effects of inhibition of miR-103 expression on the proliferation, migration, and apoptosis of NHDFs and their secretion of inflammatory cytokines under high glucose

Consistent with the aforementioned results, the apoptosis rate of NHDFs in the HG + anti-miR-103 group was significantly lower while the level of RCAN1 protein expression was obviously higher compared with the HG + anti-miR-con group ($P < 0.05$; Figure 6A-D). Moreover, compared with the HG + anti-miR-con group, the intracellular Bax protein expression was overtly lower while intracellular Bcl-2 protein expression was substantially higher in the HG + anti-miR-103 group ($P < 0.05$; Figure 6C,E,F). In addition, NHDFs in the HG + anti-miR-103 group had stronger proliferation and migration capacities significantly compared with the HG + anti-miR-con group

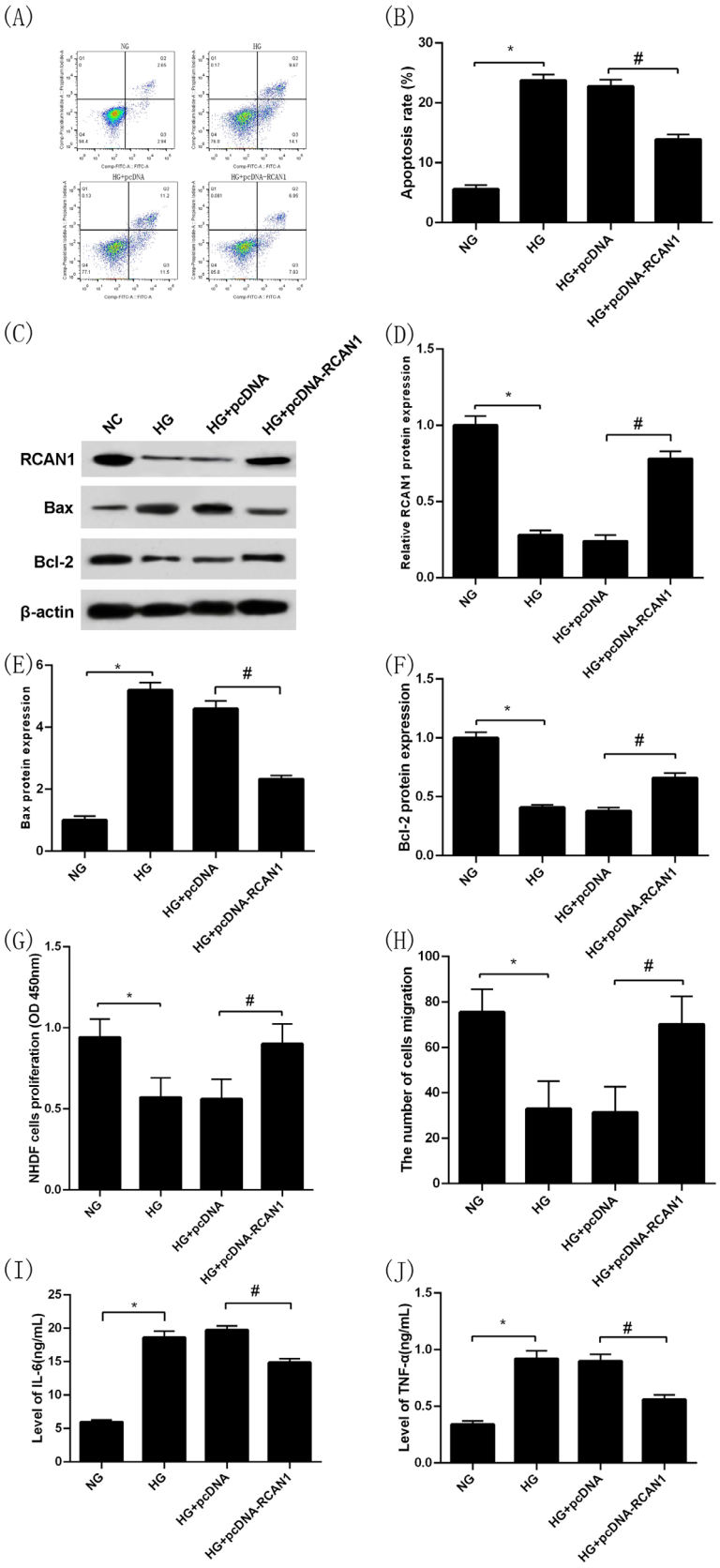

FIGURE 5 Overexpression of RCAN1 inhibits the effects of high glucose on the proliferation, migration, and apoptosis of NHDFs and secretion of inflammatory cytokines by NHDFs. Apoptosis rate of NHDFs in NC, HG, HG + pcDNA and HG + pcDNA-RCAN1 groups by flow cytometry (A),(B); RCAN1 protein expression in NC, HG, HG + pcDNA and HG + pcDNA-RCAN1 groups by Western blotting (C),(D); Bax protein expression in NC, HG, HG + pcDNA and HG + pcDNA-RCAN1 groups by Western blotting (C),(E); Bcl-2 protein expression in NC, HG, HG + pcDNA and HG + pcDNA-RCAN1 groups by Western blotting (C),(F); Proliferation capacity of NHDFs in NC, HG, HG + pcDNA and HG + pcDNA-RCAN1 groups by CCK-8 (G); The number cells of migration of NHDFs in NC, HG, HG + pcDNA and HG + pcDNA-RCAN1 groups by transwell migration assay (H); IL-6 levels in cell culture medium in NC, HG, HG + pcDNA and HG + pcDNA-RCAN1 groups by ELISA (I); TNF-α levels in cell culture medium in NC, HG, HG + pcDNA and HG + pcDNA-RCAN1 groups by ELISA (J); $^{*}P < 0.05$ vs the NG group, $^{\#}P < 0.05$ vs the HG + pcDNA group. n = 3 in each group. NG, normal glucose; HG, high glucose; NHDFs, human dermal fibroblasts; RCAN1, regulator of calcineurin 1

($P < 0.05$, Figure 6G,H). In contrast，IL-6 and TNF-α levels in cell culture medium in the HG + anti-miR-103 group were markedly lower than those in the HG + anti-miR-con group ($P < 0.05$, Figure 6I,J). At the same time, the NHDFs transfected with anti-miR-103 and si-con, anti-miR-103 and si-RCAN1 for 24 h under

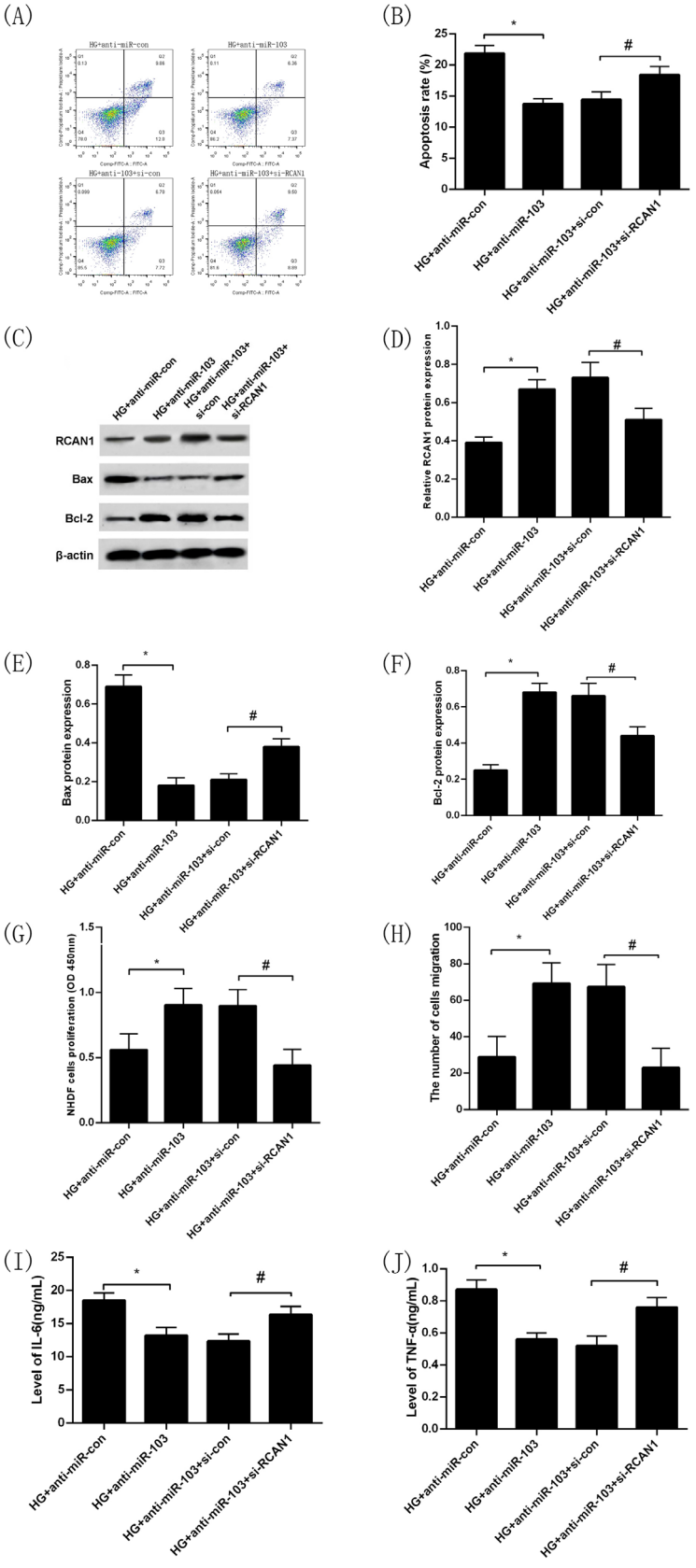

FIGURE 6 Inhibition of RCAN1 expression can reverse the protective effect of miR-103 down-regulation on the proliferation, migration, and apoptosis of NHDFs and their secretion of inflammatory cytokines under high glucose. Apoptosis rate of NHDFs in HG + anti-miR-con, HG + anti-miR-103, HG + anti-miR-103 + si-con and HG + anti-miR-103 + si-RCAN1 groups by flow cytometry (A),(B); RCAN1 protein expression in HG + anti-miR-con, HG + anti-miR-103, HG + anti-miR-103 + si-con and HG + anti-miR-103 + si-RCAN1 groups by Western blotting (C),(D); Bax protein expression in HG + anti-miR-con, HG + anti-miR-103, HG + anti-miR-103 + si-con and HG + anti-miR-103 + si-RCAN1 groups by Western blotting (C),(E); Bcl-2 protein expression in HG + anti-miR-con, HG + anti-miR-103, HG + anti-miR-103 + si-con and HG + anti-miR-103 + si-RCAN1 groups by Western blotting (C),(F); Proliferation capacity of NHDFs in HG + anti-miR-con, HG + anti-miR-103, HG + anti-miR-103 + si-con and HG + anti-miR-103 + si-RCAN1 groups by CCK-8 (G); The number cells of migration of NHDFs in HG + anti-miR-con, HG + anti-miR-103, HG + anti-miR-103 + si-con and HG + anti-miR-103 + si-RCAN1 groups by transwell migration assay (H); IL-6 levels in cell culture medium in HG + anti-miR-con, HG + anti-miR-103, HG + anti-miR-103 + si-con and HG + anti-miR-103 + si-RCAN1 groups by ELISA (I); TNF-α levels in cell culture medium in HG + anti-miR-con, HG + anti-miR-103, HG + anti-miR-103 + si-con and HG + anti-miR-103 + si-RCAN1 groups by ELISA (J). $^{*}P < 0.05$ vs the HG+ anti-miR-con group, $^{\#}P < 0.05$ vs the HG + anti-miR-103 + si-con group. n = 3 in each group. NG, normal glucose; HG, high glucose; NHDFs, human dermal fibroblasts; RCAN1, regulator of calcineurin 1

high-glucose intervention, respectively. The results showed that the apoptosis rate of NHDFs was increased and the level of RCAN1 protein expression was decreased in the HG + anti-miR-103 + si-RCAN1 compared with the HG + anti-miR-103 + si-con group ($P < 0.05$, Figure 6A-D), indicating that the transfection

was successful. The intracellular Bax protein expression level in the HG + anti-miR-103 + si-RCAN1 group was higher and the intracellular Bcl-2 protein expression level was lower than that in the HG + anti-miR-103 + si-con group, respectively ($P < 0.05$, Figure 6C,E,F). Meanwhile, NHDFs in the HG + anti-miR-103 + si-RCAN1 group had worse proliferation and migration capacities compared with the HG + anti-miR-103 + si-con group ($P < 0.05$, Figure 6G,H). Moreover, the IL-6 and TNF-α levels in cell culture medium in the HG +- anti-miR-103 + si-RCAN1 group were significantly higher than those in the HG + anti-miR-103 + si-con group ($P < 0.05$, Figure 6I,J).

4 | DISCUSSION

It is generally believed that DFU is harder to heal than non-diabetic chronic skin wounds, and hyperglycemia is an important adverse factor.[4] This study found that the expression level of miR-103 in the wound margin tissue in T2DM patients associated with DFU was significantly higher than that in patients with a chronic skin ulcer of lower limbs and normal glucose tolerance under the matching of age, gender, ulcer area, ulcer course, lower limb blood supply and systemic inflammatory response. Correlation analysis showed that the expression level of miR-103 in the wound margin tissue in DFU patients was positively correlated with the levels of blood glucose and was negatively correlated with the healing rate of foot ulcers after four weeks, and DFU with higher expression of miR-103 has a lower healing rate. In vitro experiments revealed that high glucose could upregulate the expression of miR-103 in NHDFs, thereby inhibiting the proliferation and migration of NHDFs, and promoting its apoptosis, indicating that one of the mechanisms of hyperglycemia as a detriment factor for wound repair is the up-regulation of miR-103 expression in high glucose environment, which will damage the healing of the chronic wound.

Clinically, diabetic foot ulcers are often complicated by varying degrees of wound infection and systemic inflammatory response. The Wagner classification of the DFUs selected in this study was class II-III, with mild to moderate infection status. Previous research has found that serum miR-103 expression is reduced in patients with non-infectious systemic inflammatory response syndrome and sepsis compared with healthy controls.[40] However, some studies have shown that the expression level of miR-103 is increased in the peripheral blood of patients with type 2 diabetes.[36,37] These results suggest that hyperglycemia and inflammatory responses may mutually inversely regulate the expression of miR-103 in peripheral blood. Surprisingly, in this study, the expression level of miR-103 was significantly increased in the margin tissue of infected wounds in the DFU group compared with the SUC group. Because there were no significant differences between the two groups in terms of gender, age, ulcer area, ulcer duration, and inflammatory indicators reflecting systemic inflammatory response, we believe that the difference in miR-103 expression in wound margin tissue between the two groups may be related to hyperglycemia, which may have a stronger regulatory effect on miR-103 expression than inflammatory responses. Notably, we can not explain the reason for the up-regulation of miR-103 expression in T2DM patients. However, a previous study demonstrated that high blood sugar potentially regulates the expression of miR-24 by inducing the activation of c-Myc.[41] A recent study showed that cellular reprogramming of diabetic foot ulcer fibroblasts triggers altered expression of some miRNAs associated with foot ulcer healing, thereby affecting wound healing.[42] Therefore, more studies are needed to clarify the mechanism of miR-103 expression change in a high glucose environment.

Studies have confirmed that fibroblasts are involved in each stage of wound healing, and the functions of fibroblasts may be regulated by miRNAs.[43] In order to further show the underlying mechanism of the effect of miR-103 expression changes on wound healing under high-glucose environment, in view of the importance of fibroblasts in wound healing, we selected NHDFs for in vitro experiment. This study found that in a high-glucose condition, the proliferation and migration capacities of NHDFs decreased, and the percentage of apoptotic cells increased. These results are consistent with previous studies.[6,8,9] In addition, the present study demonstrated that miR-103 expression was significantly increased in NHDFs under high glucose. Further study revealed that the inhibition of miR-103 expression could significantly increase the proliferation and migration capacities of NHDFs in a high-glucose environment, upregulate the intracellular Bcl-2 expression level, and reduce the expression level of Bax and the apoptosis rate of NHDFs. Some in vitro studies have found that down-regulation of miR-103 expression can promote the proliferation and migration of glioma cells,[44] non-small cell lung cancer cells,[45] prostate cancer cells,[46] etc. Previous studies have shown that increased Bax protein expression promotes apoptosis, while increased Bcl-2 protein expression inhibits apoptosis.[47] Thus, the aforementioned research reports strengthen our findings. At present, it is believed that the inflammatory responses in epidermal fibroblasts are closely related to their functional changes and can affect the healing process of skin wounds.[48] IL-6 and TNF-α are representative pro-inflammatory cytokines. The results of this study showed that the expression of IL-6 and TNF-α in NHDFs was significantly increased in

the high-glucose environment, indicating that the innate immunity of NHDFs was activated by high-glucose intervention to produce inflammatory responses. After the inhibition of miR-103 expression, the levels of IL-6 and TNF-α in the culture medium of NHDFs were significantly decreased, suggesting that inhibition of miR-103 expression could reduce the inflammatory responses of NHDFs under the high-glucose intervention. In the cellular Alzheimer's disease (AD) model of rat pheochromocytoma cell line PC12 cells and cellular AD model of rat cerebral cortex neurons, Yang H et al.[49] found that decreased miR-103 expression can reduce IL-1β, IL-6 and TNF-α expression levels in both two cellular AD models, supporting our findings. Collectively, the above results suggest that increased miR-103 expression might be involved in the regulation of functional impairment in dermal fibroblasts under high-glucose conditions, and then have an adverse effect on wound healing.

Previous studies have found that hyperglycemia plays an important role in the regulation of RCAN1 expression.[50,51] In the present study, we found that the mRNA expression of RCAN1 in the wound margin tissue in T2DM patients associated with DFU was significantly lower than that in patients with a chronic skin ulcer of lower limbs and normal glucose tolerance, and the protein and mRNA levels of RCAN1 were markedly decreased in high glucose-treated NHDFs. Overexpression of RCAN1 expression in NHDFs under high-glucose treatment can significantly improve the proliferation and migration capacities of NHDFs, upregulate intracellular Bcl-2 protein, and simultaneously reduce the expression levels of Bax, IL-6 and TNF-α as well as the cell apoptosis rate in the high-glucose environment. These findings indicate that decreased RCAN1 expression may play a pivotal role in NHDFs injury under high-glucose conditions. Studies have shown that decreased expression of RCAN1 is associated with abnormal mitochondrial function in type 2 diabetes,[27,28] which supports our results. However, Emrani Bidi et al. revealed that high glucose increased RCAN1 expression in C2C12 myotubes[50]; Peiris et al. also demonstrated that under chronic high glucose, the expression level of RCAN1 in pancreatic islet β cells increased 1.5 times compared with that in the control group.[51] These findings are inconsistent with our results. The specific reason is not clear, which may be related to the bidirectional regulation of RCAN1 expression in different cells by high glucose.

In this study, whether in DFU group or SUC group, we found that the mRNA expression level of RCAN1 was negatively correlated with the mRNA expression level of miR-103 in the wound margin tissue. In addition, in vitro studies revealed that the decreased protein and mRNA levels of RCAN1 in NHDFs were attenuated by the downregulation of miR-103. To further explore whether downregulation of miR-103 can prevent NHDFs impairment induced by high-glucose treatment by targeting RCAN1, we used bioinformatics prediction and a dual-luciferase reporter gene to verify that the UTR of the RCAN1 gene is a target of miR-103. Upregulating or downregulating the expression of miR-103 significantly altered RCAN1 levels, indicating that miR-103 has a negative regulatory effect on RCAN1 expression. In addition, inhibition of RCAN1 expression significantly reversed the effects of the inhibition of miR-103 expression on the proliferation, migration, and apoptosis of NHDFs and secretion of inflammatory cytokines by NHDFs under high glucose. These results indicate that up-regulation of miR-103 under high glucose conditions can lead to functional damage of NHDFs by targeted regulation of RCAN1 gene expression. In other words, interfering with miR-103/RCAN1 effect can protect NHDFs from functional impairment caused by a high-glucose environment. To our knowledge, this is the first report that miR-103 is involved in the high glucose-induced functional impairment in dermal fibroblasts through targeted regulation of RCAN1 expression.

In summary, this is the first study to find that the increased expression of miR-103 in wound tissue of DFU may be associated with poor wound healing, and demonstrate that miR-103 promotes high glucose-induced apoptosis and dysfunction in NHDFs in vitro by targeting the reduction of RCAN1 expression, so as to participate in wound healing. These may be beneficial candidates for the diagnosis and treatment of chronic wounds in diabetes.

However, there are some limitations in our study: (1) the single-centre study had a relatively small sample size, and there was an inevitable selection bias in this study, thus more research is needed to confirm the findings in our study; (2) In clinical studies, no location-matched healthy skin tissue was established as a control, making it difficult to accurately evaluate whether the change of miR-103 expression in chronic ulcer tissue is specific to wound local tissue; (3) The results of this study are derived only from biochemical and functional studies based on a two-dimensional monoculture system in vitro. If these results are extended to the therapeutic concepts, considerable limitations remain. Therefore, in the future, more studies are needed to explore target cell and tissue interactions in appropriate models in vitro and in vivo. In addition, a recent proteomic study found that under certain circumstances, dermal fibroblasts can secrete many proteins and participate in cell proliferation, adhesion, and migration, promoting wound healing.[52] Further studies should investigate whether the targeted regulation of RCAN1 by miR-103 in a high-glucose environment can also affect the expression of fibroblast-secreted proteins that promote wound healing.

AUTHOR CONTRIBUTIONS

Mingwei Chen and Youmin Wang designed the experimental scheme. Xiaotong Zhao and Murong Xu participated in the data collection and laboratory testing. Ying Tang and Dandan Xie analysed the experimental data, and Xiaotong Zhao wrote the article. Mingwei Chen critically revised the manuscript. All authors read and approved the final manuscript.

ACKNOWLEDGEMENTS

We are grateful to all patients for participating in the study. We thank the participants of this study including the doctors, nurses, and researchers from the Department of Endocrinology and the Burns Department in the First Affiliated Hospital of Anhui Medical University.

FUNDING INFORMATION

This study was supported by the Natural Science Foundation of Anhui Province in China (2108085MH269) and the Natural Science Research Project of Colleges and Universities in Anhui Province (KJ2021A0274). The funding body had no role in the design of the study, the collection, analysis, and interpretation of data, or in writing the manuscript.

CONFLICT OF INTEREST

The authors declare that they have no competing interests.

DATA AVAILABILITY STATEMENT

The datasets used and/or analysed during the current study are available from the corresponding author on reasonable request. Inquiries for data access may be sent to the following e-mail address: chmw1@163.com.

INFORMED CONSENT

Written informed consent was obtained from all the respondents.

ORCID

Xiaotong Zhao https://orcid.org/0000-0003-3736-6973
Mingwei Chen https://orcid.org/0000-0002-8439-0469

REFERENCES

1. Armstrong DG, Boulton AJM, Bus SA. Diabetic foot ulcers and their recurrence. *N Engl J Med*. 2017;376(24):2367-2375.
2. Everett E, Mathioudakis N. Update on management of diabetic foot ulcers. *Ann N Y Acad Sci*. 2018;1411(1):153-165.
3. Jiang Y, Wang X, Xia L, et al. A cohort study of diabetic patients and diabetic foot ulceration patients in China. *Wound Repair Regen*. 2015;23(2):222-230.
4. Salazar JJ, Ennis WJ, Koh TJ. Diabetes medications: impact on inflammation and wound healing. *J Diabetes Complicat*. 2016;30(4):746-752.
5. Sorg H, Tilkorn DJ, Hager S, Hauser J, Mirastschijski U. Skin wound healing: an update on the current knowledge and concepts. *Eur Surg Res*. 2017;58(1–2):81-94.
6. Almeida MES, Monteiro KS, Kato EE, et al. Hyperglycemia reduces integrin subunits alpha v and alpha 5 on the surface of dermal fibroblasts contributing to deficient migration. *Mol Cell Biochem*. 2016;421(1–2):19-28.
7. Kruse CR, Singh M, Sørensen JA, Eriksson E, Nuutila K. The effect of local hyperglycemia on skin cells in vitro and on wound healing in euglycemic rats. *J Surg Res*. 2016;206(2):418-426.
8. Senthil KK, Gokila VM, Mau JL, et al. A steroid like phytochemical Antcin M is an anti-aging reagent that eliminates hyperglycemia-accelerated premature senescence in dermal fibroblasts by direct activation of Nrf2 and SIRT-1. *Oncotarget*. 2016;7(39):62836-62861.
9. Lin HI, Chu SJ, Perng WC, Wu CP, Lin ZY, Huang KL. Hyperbaric oxygen attenuates cell growth in skin fibroblasts cultured in a high-glucose medium. *Wound Repair Regen*. 2008;16(4):513-519.
10. Lafosse A, Dufeys C, Beauloye C, Horman S, Dufrane D. Impact of hyperglycemia and low oxygen tension on adipose-derived stem cells compared with dermal fibroblasts and keratinocytes: importance for wound healing in type 2 diabetes. *PLoS One*. 2016;11(12):e0168058.
11. Moruzzi N, Del Sole M, Fato R, et al. Short and prolonged exposure to hyperglycaemia in human fibroblasts and endothelial cells: metabolic and osmotic effects. *Int J Biochem Cell Biol*. 2014;53:66-76.
12. Theocharidis G, Baltzis D, Roustit M, et al. Integrated skin transcriptomics and serum multiplex assays reveal novel mechanisms of wound healing in diabetic foot ulcers. *Diabetes*. 2020;69(10):2157-2169.
13. den Dekker A, Davis FM, Kunkel SL, Gallagher KA. Targeting epigenetic mechanisms in diabetic wound healing. *Transl Res*. 2019;204:39-50.
14. Saliminejad K, Khorram Khorshid HR, Soleymani Fard S, Ghaffari SH. An overview of microRNAs: biology, functions, therapeutics, and analysis methods. *J Cell Physiol*. 2019;234(5):5451-5465.
15. Andl T, Murchison EP, Liu F, et al. The miRNA-processing enzyme dicer is essential for the morphogenesis and maintenance of hair follicles. *Curr Biol*. 2006;16(10):1041-1049.
16. Yi R, Pasolli HA, Landthaler M, et al. DGCR8-dependent microRNA biogenesis is essential for skin development. *Proc Natl Acad Sci U S A*. 2009;106(2):498-502.
17. Etich J, Bergmeier V, Pitzler L, Brachvogel B. Identification of a reference gene for the quantification of mRNA and miRNA expression during skin wound healing. *Connect Tissue Res*. 2017;58(2):196-207.
18. Bai WL, Dang YL, Yin RH, et al. Differential expression of microRNAs and their regulatory networks in skin tissue of Liaoning cashmere goat during hair follicle cycles. *Anim Biotechnol*. 2016;27(2):104-112.
19. Wang S, Kobeissi A, Dong Y, et al. MicroRNAs-103/107 regulate autophagy in the epidermis. *J Invest Dermatol*. 2018;138(7):1481-1490.
20. Han LL, Yin XR, Zhang SQ. miR-103 promotes the metastasis and EMT of hepatocellular carcinoma by directly inhibiting LATS2. *Int J Oncol*. 2018;53(6):2433-2444.

21. Zhao Y, Gu X, Wang Y. MicroRNA-103 promotes nasopharyngeal carcinoma through targeting TIMP-3 and the Wnt/β-catenin pathway. *Laryngoscope*. 2020;130(3):E75-E82.
22. Byun JS, Gardner K. Wounds that will not heal: pervasive cellular reprogramming in cancer. *Am J Pathol*. 2013;182(4):1055-1064.
23. Norberg KJ, Nania S, Li X, et al. RCAN1 is a marker of oxidative stress, induced in acute pancreatitis. *Pancreatology*. 2018;18(7):734-741.
24. Fu Q, Wu Y. RCAN1 in the inverse association between Alzheimer's disease and cancer. *Oncotarget*. 2017;9(1):54-66.
25. Peiris H, Keating DJ. The neuronal and endocrine roles of RCAN 1 in health and disease. *Clin Exp Pharmacol Physiol*. 2018;45(4):377-383.
26. Chen HM, Dai JJ, Zhu R, et al. RCAN1.4 mediates high glucose-induced matrix production by stimulating mitochondrial fission in mesangial cells. *Biosci Rep*. 2020;40(1):BSR20192759.
27. Peiris H, Dubach D, Jessup CF, Unterweger P, Raghupathi R, Muyderman H, Zanin MP, Mackenzie K, Pritchard MA, Keating DJ RCAN1 regulates mitochondrial function and increases susceptibility to oxidative stress in mammalian cells. *Oxidative Med Cell Longev* 2014;2014:520316, 1, 12.
28. Fadista J, Vikman P, Laakso EO, et al. Global genomic and transcriptomic analysis of human pancreatic islets reveals novel genes influencing glucose metabolism. *Proc Natl Acad Sci U S A*. 2014;111(38):13924-13929.
29. Li H, Zhang W, Zhong F, et al. Epigenetic regulation of RCAN1 expression in kidney disease and its role in podocyte injury. *Kidney Int*. 2018;94(6):1160-1176.
30. Kim SS, Kim NK, Seo SR. Cynanchi atrati and its phenolic constituent sinapic acid target regulator of calcineurin 1 (RCAN1) to control skin inflammation. *Antioxidants (Basel)*. 2022;11(2):205.
31. Ballesteros-Martinez C, Mendez-Barbero N, Montalvo-Yuste A, et al. Endothelial regulator of calcineurin 1 promotes barrier integrity and modulates histamine-induced barrier dysfunction in anaphylaxis. *Front Immunol*. 2017;8:1323.
32. Gimeno A, García-Giménez JL, Audí L, et al. Decreased cell proliferation and higher oxidative stress in fibroblasts from down syndrome fetuses. *Preliminary Study Biochim Biophys Acta*. 2014;1842(1):116-125.
33. Vistejnova L, Safrankova B, Nesporova K, et al. Low molecular weight hyaluronan mediated CD44 dependent induction of IL-6 and chemokines in human dermal fibroblasts potentiates innate immune response. *Cytokine*. 2014;70(2):97-103.
34. Shaw TJ, Martin P. Wound repair: a showcase for cell plasticity and migration. *Curr Opin Cell Biol*. 2016;42:29-37.
35. Vatandoost N, Amini M, Iraj B, Momen-zadeh S, Salehi R. Dysregulated miR-103 and miR-143 expression in peripheral blood mononuclear cells from induced prediabetes and type 2 diabetes rats. *Gene*. 2015;572(1):95-100.
36. Ghasemi H, Karimi J, Khodadadi I, Tavilani H. Correlation between miR-103 and miR-133a expression and the circulating ANGPTL8 in type 2 diabetic patients and healthy control subjects. *Clin Lab*. 2019;65(11).
37. Luo M, Xu C, Luo Y, Wang G, Wu J, Wan Q. Circulating miR-103 family as potential biomarkers for type 2 diabetes through targeting CAV-1 and SFRP4. *Acta Diabetol*. 2020;57(3):309-322.
38. Vienberg S, Geiger J, Madsen S, Dalgaard LT. MicroRNAs in metabolism. *Acta Physiol (Oxf)*. 2017;219(2):346-361.
39. Li X, Tang Y, Jia Z, Zhao X, Chen M. Decreased expression of miR-24 in peripheral plasma of type 2 diabetes mellitus patients associated with diabetic foot ulcer. *Wound Repair Regen*. 2020;28(6):728-738.
40. Yang M, Zhao L, Sun M. Diagnostic value of miR-103 in patients with sepsis and noninfectious SIRS and its regulatory role in LPS-induced inflammatory response by targeting TLR4. *Int J Genomics*. 2020;2020:2198308.
41. Xiang Y, Cheng J, Wang D, et al. Hyperglycemia repression of miR-24 coordinately upregulates endothelial cell expression and secretion of von Willebrand factor. *Blood*. 2015;125(22):3377-3387.
42. Pastar I, Marjanovic J, Liang L, et al. Cellular reprogramming of diabetic foot ulcer fibroblasts triggers pro-healing miRNA-mediated epigenetic signature. *Exp Dermatol*. 2021;30(8):1065-1072.
43. Jhamb S, Vangaveti VN, Malabu UH. Genetic and molecular basis of diabetic foot ulcers: clinical review. *J Tissue Viability*. 2016;25(4):229-236.
44. Chen LP, Zhang NN, Ren XQ, He J, Li Y. miR-103/miR-195/miR-15b regulate SALL4 and inhibit proliferation and migration in glioma. *Molecules*. 2018;23(11):2938.
45. Yang D, Wang JJ, Li JS, Xu QY. miR-103 functions as a tumor suppressor by directly targeting programmed cell death 10 in NSCLC. *Oncol Res*. 2018;26(4):519-528.
46. Fu X, Zhang W, Su Y, Lu L, Wang D, Wang H. MicroRNA-103 suppresses tumor cell proliferation by targeting PDCD10 in prostate cancer. *Prostate*. 2016;76(6):543-551.
47. Dolka I, Król M, Sapierzyński R. Evaluation of apoptosis-associated protein (Bcl-2, Bax, cleaved caspase-3 and p53) expression in canine mammary tumors: an immunohistochemical and prognostic study. *Res Vet Sci*. 2016;105:124-133.
48. Barrientos S, Stojadinovic O, Golinko MS, Brem H, Tomic-Canic M. Growth factors and cytokines in wound healing. *Wound Repair Regen*. 2008;16(5):585-601.
49. Yang H, Wang H, Shang H, et al. Circular RNA circ_0000950 promotes neuron apoptosis, suppresses neurite outgrowth and elevates inflammatory cytokines levels via directly sponging miR-103 in Alzheimer's disease. *Cell Cycle*. 2019;18(18):2197-2214.
50. Emrani Bidi R, Rebillard A, Saligaut D, Delamarche A, Davies KJA, Cillard J. Acute electrical pulse stimulation and hyperglycemia regulates RCAN1-4 in C2C12 myotubes through oxidative stress. *Free Radic Biol Med*. 2014;75(Suppl 1):S29.
51. Peiris H, Raghupathi R, Jessup CF, et al. Increased expression of the glucose-responsive gene, RCAN1, causes hypoinsulinemia, β-cell dysfunction, and diabetes. *Endocrinology*. 2012;153(11):5212-5221.
52. Maarof M, Lokanathan Y, Ruszymah HI, Saim A, Chowdhury SR. Proteomic analysis of human dermal fibroblast conditioned medium (DFCM). *Protein J*. 2018;37(6):589-607.

How to cite this article: Zhao X, Xu M, Tang Y, Xie D, Wang Y, Chen M. Changes in miroRNA-103 expression in wound margin tissue are related to wound healing of diabetes foot ulcers. *Int Wound J*. 2023;20(2):467-483. doi:10.1111/iwj.13895